THE BULLETIN OF OKAYAMA UNIVERSITY OF SCIENCE No. 50 A pp. 23-32(2014)

Capillary zone electrophoretic separation of carbon microparticles

Takashi Yokoyama, Yuta Shiraishi*, Keiji Tada*, Wakako Masuda, Masaaki Sugiyama,

Akira Maekawa, and Michio Zenki

Department of Chemistry, Faculty of Science,
**Graduate School of Science,*
Okayama University of Science,
1-1 Ridai-cho, Kita-ku, Okayama 700-0005, Japan

(Received September 8, 2014; accepted November 6, 2014)

Capillary zone electrophoretic separations of carbon particles in micrometer and submicrometer sizes were achieved in an aqueous 10 mM sodium tetraborate solution containing 10%(w/v) polyethylene glycol 400 at pH 9.2 as background electrolyte solution (BGE). Since migration time of the carbon particle increased with increasing its size, it was shown that the larger size of the carbon particle had a more negatively electric charge. Electropherograms corresponded to histograms of size distributions from images observed by scanning electron microscope (SEM) or a digital microscope. The size distribution could be measured within 20 min by capillary electrophoresis (CE). This means that the generally well-used SEM could be replaced by CE for measurements of size distributions for the carbon particles in micrometer and submicrometer, because the CE measurement could be easier than SEM at a shorter time. Also, a surface density of electric charge for a graphitic carbon microparticle of a 3.6 μm diameter was obtained from electrophoretic mobility measured by CE. It was -1.1 × 10^{-5} C m^{-2} at 30°C. Since this value would depend on numbers of proton-dissociating carboxyl and phenol groups on the carbon microparticle in BGE, it could be used as an index to estimate oxidized carbons on the surface of carbon microparticles.

Keywords: capillary electrophoresis; carbon microparticle; electrophoretic mobility; size distribution; surface density of electric charge.

1. Introduction

A number of investigations for separation of nano- and microparticles have recently been reviewed.[1)-15)] Size exclusion chromatography, field flow fractionation (FFF), and capillary electrophoresis (CE) have mainly been applied to these investigations. Since these retention or migration times and peak widths depend on these diameters and size distribution, respectively, those values are useful for characterization of sizes and concentrations of the nano- or microparticles. Although these separations have been achieved, these have not been obtained a satisfactory peak resolution. CE has also been applied to the separation of nanoparticles, such as gold, silver, metal oxides, quantum dots, colloids, polymers, liposomes, and viruses.[1)-15)] These separations of the nanoparticles have been achieved. On the other hand, applications of CE to separations of a few kinds of microparticles, which are microorganisms, such as mitochondria, bacteria, and biological cells, and aerosol particles, have been reported,[3),10),16)-22)] although generally useful capillary tubes of inner diameters from 50 to 100 μm are considered to be too narrow for the separation of the microparticles. It is

suggested that the microorganisms would migrate one by one in the capillary tube. However, their separation mechanism has not been obvious. Therefore, the electrophoretic behavior of the microparticles in the capillary tube is of interest.

Generally, sizes of 2 – 10 μm of microparticles, such as silica gel, octadecyl silica gel, synthetic polymer, and graphitic carbon, have generally been applied as packing materials of column in liquid chromatography (LC). It is also very important for those manufacturers to control a quality for these sizes and shapes of the microparticles, because a packing column using different sizes and shapes of the microparticles often gives a poor separation for analytes. The size and shape of packing materials could be generally characterized from images of scanning electron microscope (SEM) and a transmission electron microscope (TEM). It is needed to acquire great skill for the SEM and TEM measurements. Furthermore, those sample preparations are troublesome and spend a long time. Therefore, it is required to observe a size distribution of microparticles via an easy sample preparation and a fast measurement. Since CE could relatively conduct the faster measurement and the easier sample preparation, it is interesting to investigate the CE measurement for the size distribution of microparticles.

Carbons have been used as industrial sources of various carbon products, such as an activated carbon, an electrode and a capacitor. Also, many carbon-based nanomaterials, such as fullerene, carbon nanotube, graphene, and carbon dots, have recently been applied to a field in analytical chemistry.[23)-32)] Carbon microparticles have been used as packing materials of LC known as a graphitic carbon column. These carbon particles are generally prepared from combustion of organic materials. The combustion produces many alcohols, phenols, ethers, ketones, aldehydes, and carboxyl groups oxidized many carbons on surface of the carbon particles. Especially, these phenols and carboxyl groups cause a negatively electric charge of the carbon particles in an aqueous solution. Therefore, the carbons inhibit different chemical properties dependent on size, shape, surface condition and impurity. For example, although carbons do not generally inhibit fluorescence and are insoluble in water, carbon nanoparticles of diameter of *ca.* 1 nm inhibit fluorescence and are soluble in water.[25),31),33)] This is suggested by a reason why many hydrophilic hydroxyl and carboxyl groups exist on surface of these carbon particles. Accordingly, it is very important for the manufactures to control those qualities and to explore the surface conditions.

A separation of carbons is one method to control the quality of carbon particles. In case of carbons in nanometer size, their separations have been investigated by CE, FFF, LC, and sedimentation. CE generally produces a high resolution of analytes, comparing to FFF, LC, and sedimentation. The CE separations of graphene oxide and chemically converted graphene,[34),35)] chemically modified fullerenes,[36)] single-walled carbon nanotubes,[37)] and carbon nanoparticles[38)] have been reported. The peak resolution and electrophoretic mobilities (μ_{ep}) of the various carbon nanomaterials of different surface conditions, sizes, shapes and impurities are useful for an evaluation to characterize these properties. However, the carbon nanomaterials have shown a broad peak and their CE separations have not been obtained a satisfactory peak resolution. Therefore, a further CE investigation would be needed to estimate the surface conditions, sizes, and shapes of the individual carbon nanomaterials.

In case of carbons in micrometer size, separation of graphene oxide sheets has been reported by sedimentation.[39)] A separation of carbon particles in the micrometer size has not been applied to CE. However, it is expected that the carbon micromaterials might migrate one by one like microorganisms or that these populations in the capillary tube might depend on the size distribution in a sample. Therefore, the CE separation might be useful for measurement of size distribution of carbon microparticles. Furthermore, an electrophoretic behavior of relatively large carbon microparticles in *ca.* 100 μm i.d. capillary of limited space is interested. Accordingly, the CE separation of the carbon microparticles was investigated.

2. Experimental

2-1 Apparatus

CE measurements were carried out on a CAPI-3200 instrument (Otsuka Electron., Osaka, Japan), equipped with a UV-visible absorbance

detector, and an autosampler in a thermostated room. A 500 mm long (378 mm to detector cell), 75 μm i.d. fused silica capillary (GL Science, Tokyo) was used. All measurements were performed at 30°C. Sample injection was carried out in the hydrodynamic mode, while keeping the capillary end at 25 mm height for 180 s, unless otherwise stated. The applied voltage used was 20 kV, unless otherwise stated. Carbons were monitored at 600 nm on side of cathode, because any water-soluble impurities like aromatic compounds in the carbons were not detected at this wavelength.

Carbons were characterized by a SEM JSM-6490 (JEOL, Tokyo), a digital microscope VHX-1000 (Keyence, Osaka, Japan), or a TEM H8100 (Hitachi, Tokyo).

The viscosity and density of background electrolyte solution (BGE) at 30.0 ± 0.1°C were measured using an Ostwald viscometer and a Density/Specific Gravity Meter DA-110 (Kyoto Electron., Kyoto, Japan), respectively.

2-2 Reagents and materials

The reagent grade sodium tetraborate was purchased from Nacalai Tesque (Kyoto, Japan). Polyethylene glycol (PEG) 200, 400, 1000, 2000, and 6000 were purchased from Wako (Osaka, Japan). Porous graphitic carbon particles 3 (A), 5 (B), and 7 μm (C) were pulled out from Hypercarb column (Thermo Scientific, Waltham, MA), and grassy, spherical carbon powder 2 – 12 μm (D) and graphitized carbon black nanopowder <500 nm (E) were purchased from Sigma-Aldrich (St. Louis, MO), where the symbols A – E for these carbon particles are used. Various non-spherically broken carbons of 3, 4, 6, 7, 11 and 15 μm were gifted from Kuraray (Kurashiki, Japan). The symbol F for the non-spherical broken carbon of 7 μm is used.

Carbon submicroparticles were prepared by heating 4 g of glucose (Wako) dissolved in 20 ml of water in a Teflon crucible put on a lid at 180°C for 5 (G), 10 (H), 15 (I), and 20 h (J), where the symbols G – J for these prepared carbon submicroparticles are used, isolating carbon particles by centrifugation at 5000 rpm for 20 min, washing by water and ethanol, and drying at 80°C for 8 h, according a published preparation method.[40),41)]

All water was purified using a Milli-Q water system (Millipore, Bedford, MA), after distillation through a mixed ion-exchange resin column.

2-3 Procedure

The capillary was first conditioned with 1 M NaOH for 3 min. It was automatically washed with water for 3 min and rinsed with BGE for 3 min between runs. The BGE, which was prepared from PEG 400 and aqueous sodium tetraborate solution, was filtrated through a 0.45 μm hydrophilic polytetrafluoroethylene filter (Advantec, Tokyo), before using. A small dip peak due to a small difference of refractive indeces between sample and BGE or acetophenone was used as an electroosmotic flow (EOF) marker. The time of the dip peak corresponded to migration time of acetophenone well-used as the EOF marker. The sample solutions were prepared as the 500 μg mL^{-1} solution distributed the carbons into BGE, unless otherwise stated. The μ_{ep} values were calculated from an equation (1)

$$\mu_{ep} = l_d l_t (t^{-1} - t_0^{-1}) V^{-1} \qquad (1),$$

where l_d, l_t, t, t_0, and V are the capillary length to detector, the total capillary length, the migration time of carbon, the EOF time, and the applied voltage, respectively.[42)]

3. Results and discussions

3-1 Characterization of carbons

Figure 1 shows typical SEM, digital microscope

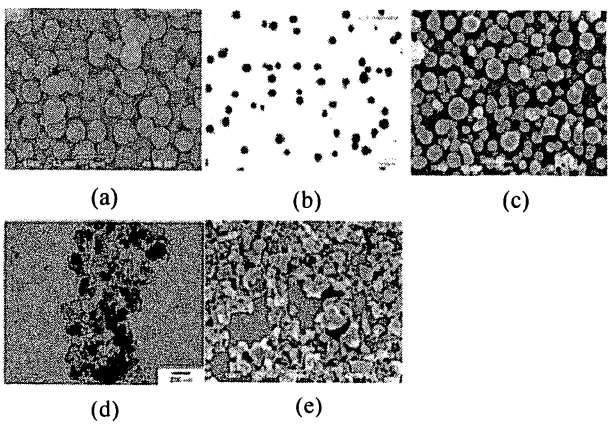

Figure 1. SEM, digital microscope, or TEM images of carbons. Carbon particles: A (a), B (b), D (c), and E (d); non-spherically broken carbons: F (e). The carbons of the symbols (a), (c) and (e), (b), and (d) were measured by SEM, digital microscope, and TEM, respectively.

or TEM images of carbon particles A, B, D, E, and non-spherically broken carbons F. Digital microscope image of carbon particles C was nearly the same as B. Almost all these carbon particles of A – E were spherical. The non-spherically broken carbons F of 7 μm were various shapes and sizes. The SEM images for the other non-spherical broken carbons of 3, 4, 6, 11, and 15 μm, which were measured as probably medians by the manufacturer, were almost the similar to those for F. These average diameters of the non-spherical broken carbons measured from the SEM images by a scale in this work were 6.1 ± 2.8 (n = 579), 5.0 ± 2.6 (490), 4.2 ± 2.5 (1095), 4.4 ± 2.5 (1065), 6.3 ± 4.3 (1190), and 7.8 ± 5.6 μm (1492), respectively, where n is number of the carbons measured from the SEM images by a scale, error is standard deviation, and the longest diameters of non-spherically broken carbons were measured as each of the diameters. Since the deviations of these average diameters were large, F of 4.4 ± 2.5 μm was mainly used in CE measurements as the representative non-spherically broken carbons. Figure 2 shows typical SEM images of prepared carbon submicroparticles. Although these shapes were spherical, many carbon submicroparticles were stuck together.

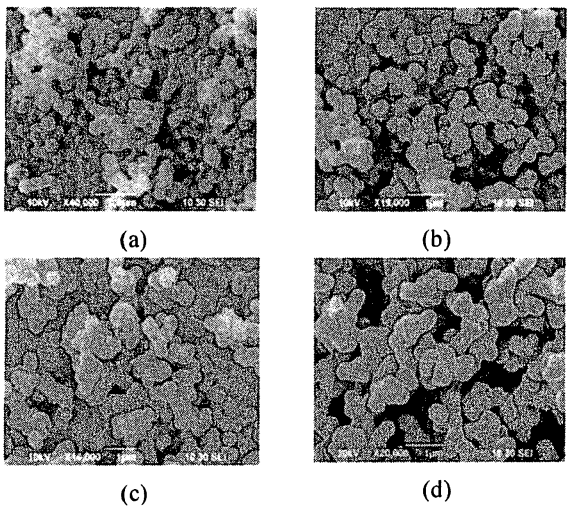

(a) (b) (c) (d)

Figure 2. SEM images of prepared carbon submicroparticles. Prepared carbon submicroparticles: G (a), H (b), I (c), and J (d).

The average diameters of the carbons A – J measured from the microscope images are summarized in Table 1. The deviations of the average diameters for the carbons A – C, G and H were relatively small, compared to those of D – F, I and J. The average diameters of the prepared carbon submicroparticles increased with increasing the heating time to prepare them.

Table 1 Average diameters of carbons measured from microscope images

Carbon	Average diameter / μm[1)]	n[2)]
A	3.2 ± 0.8	232
B	5.6 ± 0.7	133
C	5.7 ± 0.7	100
D	3.9 ± 1.2	292
E	0.044 ± 0.017	165
F	4.4 ± 2.5	1065
G	0.17 ± 0.03	100
H	0.41 ± 0.06	100
I	0.53 ± 0.18	100
J	0.75 ± 0.27	100

[1)] Error is standard deviation. [2)] n is number of carbons measured from microscope images by a scale.

Figure 3 shows typical histograms on size distributions of these carbon particles A, B, D and E. An obviously sharp mode (the largest population) of 3.6 μm was found in the histogram of the carbon microparticles A. On the other hands, the obviously sharp mode was not found in the histograms of carbon microparticles B, C and D. The wide range of sizes was found in the histogram of carbon nanoparticles E.

3-2 Dispersion medium of carbons

Some surfactants have generally been used as the dispersion medium of nanoparticles, such as gold nanoparticles.[43)] Halogenized solvents and heavy metal salts have often been used as additives to prepare a density of solution. Therefore, aqueous solutions of some cationic, anionic, and neutral surfactants, such as cetyltrimethylammonium bromide (CTAB), sodium dodecylsulfate (SDS), sodium n-dodecylbenzenesufonate (DBS), and Brij 58, of PEG 400, and of zinc sulfate, and 1-methyl-2-pyrolidone solutions containing halogenized solvent, as the dispersion medium of sample to prevent coagulations and precipitation of the carbons, were investigated. The carbons of F in micrometer dispersed in the dispersion media

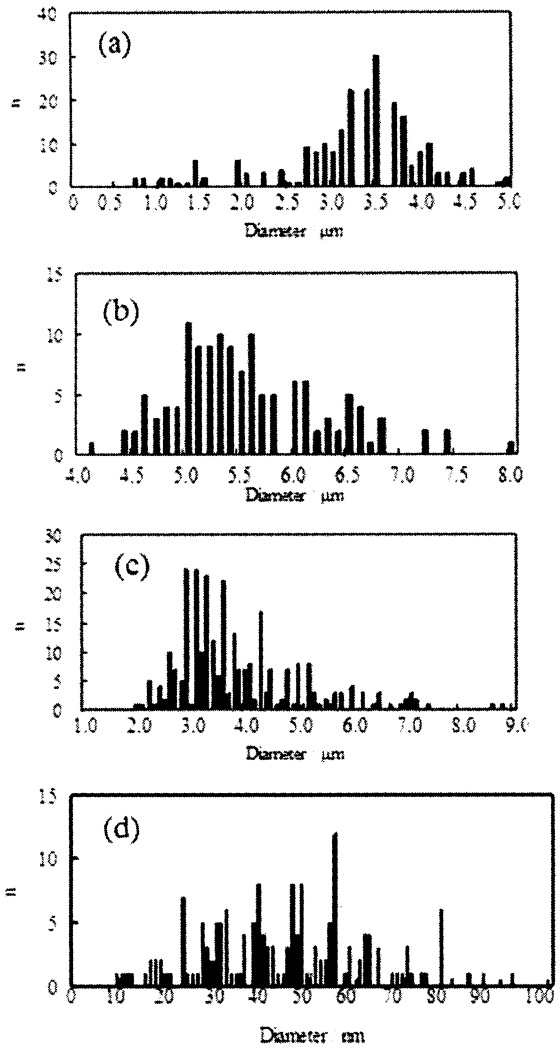

Figure 3. Histograms on size distributions of carbon particles measured from microscope images. Carbon particles: A (a), B (b), D (c), and E (d).

were stood in test tubes at room temperature. The media dispersing the carbons F for above several hours were as follows: aqueous solution of near saturated 35%(w/v) zinc sulfate, 0.01 – 0.07 M CTAB aqueous solution, 50 – 80%(w/v) PEG 400 aqueous solution, and 1-methyl-2-pyrolidone solutions of >90%(v/v) 1,3-dibromopropane. On the other hands, the media occurred precipitations of the carbons F were as follows: 0.01 – 0.1 M SDS aqueous solution, 1.2×10^{-3} – 9.6×10^{-3} M DBS aqueous solution, 7.8×10^{-5} – 0.01 M Brij 58 aqueous solution, and mixed solutions of 1-methyl-2-pyrolidone with chloroform or carbon tetrachloride. The anionic and neutral surfactants could not succeed in the dispersion of the carbons in micrometer. The high concentration of cationic surfactant CTAB solution produced precipitants of the carbons, because the carbons have negatively electric charges in the aqueous solution. Since it is considered that CTAB would form ionic associates with the carbons even in the low concentration of CTAB solution, it could not be used as the dispersion medium. The 35%(w/v) zinc sulfate solution which has a high ionic strength would cause to occur a large joule heat during a measurement of CE. Also, the high concentration of 1,3-dibromopropane in 1-methyl-2-pyrolidone solution could not produce EOF to require for the measurement of CE, because it has the very low relative permittivity. Therefore, these were not also used as the dispersion medium. Finally, the various PEG solutions were investigated in detail. The larger molecular weight and the higher concentration of PEG were, the longer dispersion life time of the carbons in micrometer was observed. Although the aqueous solutions of >20%(w/v) PEG 2000 and 6000 and of >60%(w/v) PEG 200 and 400 could disperse the carbons in micrometer for >24 hours, it was difficult to introduce these solutions into a 75 μm i.d. capillary for too high viscosity of these solutions. When the aqueous sodium tetraborate solutions with 40 – 50%(w/v) PEG 200 and 400 were used as BGE for CE, EOF became very slow. Therefore, it would spend a long time for the CE measurement of the carbons. Resultantly, the aqueous sodium tetraborate solution containing 10%(w/v) PEG 400 observed the dispersion life time of the carbons for several hours was used as the dispersion medium for both of sample and BGE, because the carbons in micrometer could be dispersed during the CE measurements and the proper EOF was available.

3-3 CE separation of carbons

Some conditions of kinds of electrolyte (sodium dihydrogen phosphate, disodium hydrogen phosphate, trisodium phosphate, and sodium tetraborate) in BGE, concentrations of the electrolyte (5 – 20 mM) and PEG 400 (0 – 30%(w/v)), pH (pH 4.5 – 11.8), applied voltage (10 – 25 kV), and sample injection time (30 – 180 s) for CE separation of carbon microparticles were investigated. When an aqueous 10 mM sodium teraborate solution containing 10%(w/v) PEG 400 at pH 9.2 as BGE, 20 kV as the applied voltage, 180 s as the sample injection time were used, good

reproducibilities of electropherograms for the carbon microparticles A – C were available. However, the good reproducibility of electropherogram for the non-spherically broken carbon F was not available. In many cases of the CE measurements, the capillary tube was clogged by F. These would be reasons why these had the various shapes and a wide micrometer range of size distributions, as the SEM image shown in Fig. 1 (e). Also, these would be broken during the CE measurements, because these physical strengths were very weak. In cases of the other non-spherically broken carbons, the results were the same as those of F.

Figure 4 shows typical electropherograms of the carbon microparticles A, B, and D, where the electropherogram of the carbon microparticles C was almost the similar to that of B, because the average diameter of C was almost the same to that of B in Table 1. A number of sharp peaks of the carbon microparticles were observed on the electropherograms of A – D in micrometer size. The reproducibility of the electropherogram of E in nanometer size was poor, because the carbon E included various shapes with the spherical carbon nanoparticles and had the relatively large nanometer size distribution, as the image shown in Fig. 1 (d). Sharp and narrow peaks were observed for the carbon microparticles, although broad peaks have generally been observed for nanoparticles, such as gold and silver. In case of the particles in nanometer size, when many nanoparticles of almost the similar sizes could pass through a cell pass of 75 μm i.d. capillary, these peaks would be broad according to a normal distribution of the sizes. The nanoparticles of largely different sizes could be separated from each other. In case of the particles in micrometer size, only small population of microparticles could pass it through. For example, only the 15 microparticles as the largest population can stand in line on the cell pass of 75 μm i.d. for a 5 μm particle. Therefore, the peaks of the particles in the micrometer size were largely different from those in the nanometer size according to the normal distribution of the sizes. Each of the sharp peaks would be due to the individual carbon microparticles in the different micrometer sizes.

Generally, a migration time of an anionic solute toward a cathode decreases with increasing its size (hydrodynamic radius), because its μ_{ep} value is in

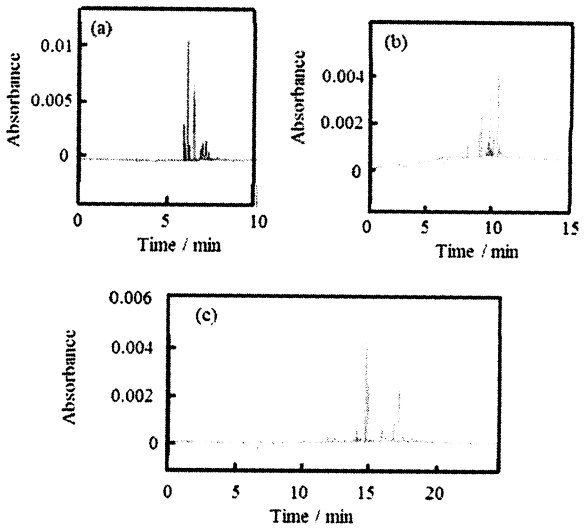

Figure 4 Electropherograms of carbon microparticles. Carbon microparticles: A (a), B (b) and D (c). Applied voltage: 20 kV; sample injection: 25 mm and 180 s; BGE: aqueous 10 mM sodium tetraborate solution containing 10%(w/v) PEG 400 at pH 9.2; sample: 500 μg mL^{-1} in BGE.

inverse proportion to its size (hydrodynamic radius).[42] However, the migration time of the larger carbon particle was longer than that of the smaller carbon particle in the micrometer size. Since the hydration of the hydrophobic carbon microparticle would be weak, it is considered that the hydrodynamic radius would be almost the similar to the size of carbon microparticles without the hydration. In other words, thickness of the hydration would be negligible, compared to the very large size of the carbon microparticle. Therefore, the negatively electric charge of the carbon microparticle might increase with increasing its size.

Each of the electropherograms in Fig. 4 was almost the similar to each of the corresponding histograms on size distribution of carbon particles in micrometer size observed from microscopes in Fig. 3. This means that the electropherogram could obtain the size distribution of microparticles observed from the microscopes. In other words, the size distribution of microparticles could be observed by CE without the microscopes. Figure 5 shows an electropherogram and a histogram of mixture of carbon microparticles A – C. The electropherogram completely corresponded to the histogram on size distribution. The highest peak would correspond to that of a

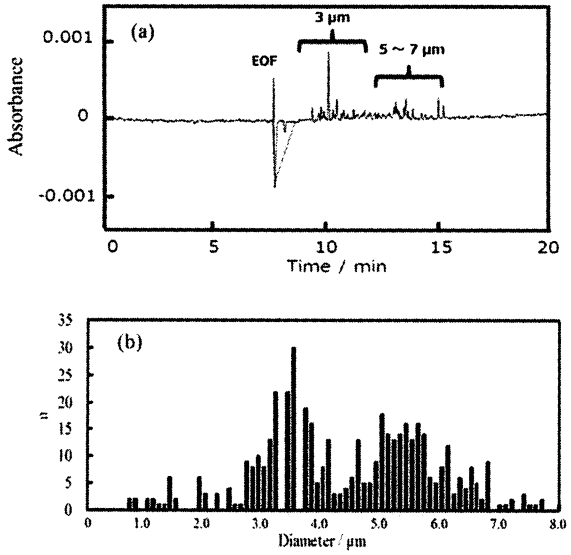

Figure 5. Electropherogram (a) and histogram (b) of mixtures of carbon microparticles A – C. Concentrations of carbon microparticles A, B, and C were 500 μg mL^{-1} each. Other conditions as in Fig. 4.

diameter of the largest population of the carbon microparticles. The corresponding diameter was 3.6 μm from Fig. 3 (a) or Fig. 5 (b). Therefore, each of the migration times of the carbon microparticles could be related to each of the diameters of the carbon microparticles.

Figures 6 and 7 show typical electropherograms and histograms of the prepared carbon submicroparticles G and I, respectively. Only a broad peak was observed on the electropherogram of carbon submicroparticle G of 170 nm in the smallest nanometer size in this work. The size deviation of G was relatively small in Table 1. It is considered that both of the small size deviation and the small submicroparticle size of G produced the broad peak. In case of I of 530 nm larger than G, many sharp peaks on a broad peak were observed. The combination of broad and sharp peaks might be due to a co-migration of the relatively large carbon submicroparticles (sharp peaks) with the relatively small carbon submicroparticles (broad peak) coexisted in I. The many sharp peaks would show that some monodispersive carbon submicroparticles migrated without their coagulation, because the whole image for the sharp peaks on the electrophergram nearly corresponded to the whole image of the histogram of size distribution for I in Fig. 7 (b), as the case of carbon microparticles. The results of the carbon submicroparticles H and J were almost the similar to that for I.

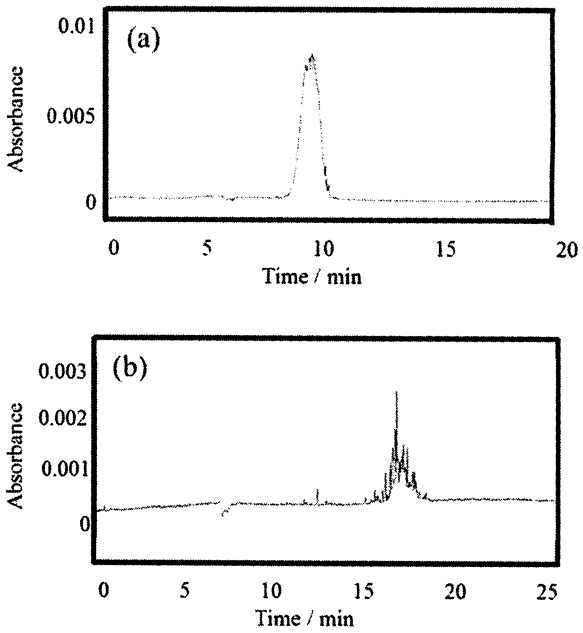

Figure 6. Electropherograms of prepared carbon submicroparticles. Prepared carbon saubmicroparticles: G (a) and I (b). Other conditions as in Fig. 4.

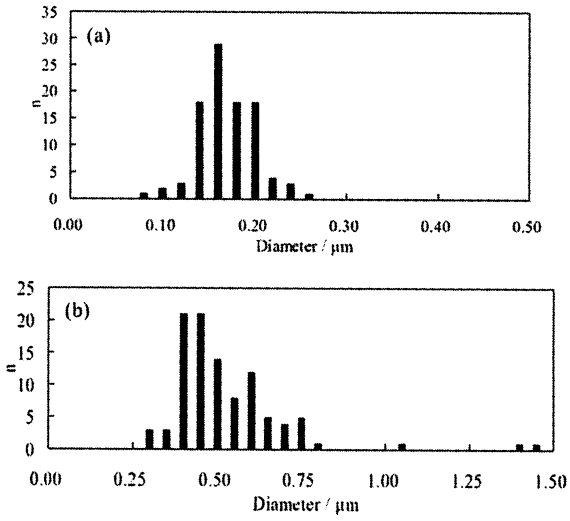

Figure 7. Histograms on size distributions of prepared carbon submicropartilces. Prepared carbon submicroparticles: G (a) and I (b).

3-4 Surface density of electric charge of carbon microparticle

The μ_{ep} value depends on both size and electric charge of solute from equation (2)

$$\mu_{ep} = q / 6\pi\eta r \qquad (2),$$

where q, η, and r are the electric charge of solute (the apparent electric charge of carbon particle), the BGE viscosity, and the solute (carbon particle) radius, respectively.[42] It has been reported that the equation (2) could not apply to nanoparticles.[44] In case of the carbon microparticles, since it is considered that thickness of hydration would be negligible, due to the very large size of microparticle and a weak hydration of hydrophobic carbon microparticles, it can be assumed that the equation (2) can apply to the carbon microparticles. Furthermore, since the radius of carbon microparticle is very larger than water and PEG molecules and ions in BGE, an increase of the radius due to an ion association, the hydration, and an adsorption between carbon microparticle and ions, water or PEG molecules in BGE would be negligible. Therefore, the half diameter of spherical carbon microparticle observed from microscope image could be used as the r value. The r value of the largest population of carbon microparticle on histogram of size distribution would correspond to the highest peak on the corresponding electropherogram. Therefore, the half diameter of the largest population of the carbon microparticle A on histogram in Fig. 3 (a) was used. The r value was 1.8 μm. Also, the μ_{ep} value was calculated from a migration time of the highest peak in Fig. 4 (a) for the carbon microparticle A by eqn (1). The μ_{ep} value was -1.07×10^{-4} cm^2 V^{-1} s^{-1}. The density and viscosity of water at 30°C used are 0.99565 g cm^{-3} and 0.7977 mPa s, respectively.[45] The BGE density and viscosity measured at 30.0 ± 0.1°C were 1.0150 g cm^{-3} and 1.202 mPa s, respectively. Therefore, an apparent electric charge of the carbon microparticle A, which was spherical in Fig. 1 (a), was calculated from eqn (2). The apparent q value was -4.4×10^{-16} C. As the carbon microparticle A was spherical, the surface density of electric charge of A was -1.1×10^{-5} C m^{-2}. Since it is considered that the negative surface density of electric charge would be related to numbers of proton-dissociating phenols and carboxyl groups existing on the surface of the carbon microparticle in BGE, the surface density of electric charge would depend on methods and source materials to prepare the carbon microparticles, pH and interactions of BGE with the carbon microparticles. However, the value could be used as an index of surface conditions for the carbon microparticle.

The μ_{ep} values of carbon microparticle B prepared by the same manufacturer were observed in range of -2.20×10^{-4} to -2.32×10^{-4} cm^2 V^{-1} s^{-1} in Fig. 3 (b). The average diameter of the carbon microparticle B was 5.6 μm in Table 1. Therefore, the apparent q values were approximately in range of -1.4×10^{-15} to -1.5×10^{-15} C from eqn (2). The apparent q values of the larger size of the carbon microparticle B were obviously smaller than the carbon microparticle A. Therefore, B was more negative than A. The apparent q value became more negative with increasing the size of carbon microparticle. The numbers of dissociating phenols and carboxyl groups would increase with increasing with the size of carbon microparticle in BGE. In other words, the oxidized surface area of carbons on carbon microparticle would increase with increasing the size of the carbon microparticle. Consequently, the larger size of carbon microparticle migrated faster toward an anode (longer migration time).

The surface density of electric charge of B was approximately -1.5×10^{-5} C m^{-1} from the apparent q values. The surface density of electric charge of B was near to A. Since both of A and B were prepared as a graphitic carbon microparticle by the same manufacturer, the surface conditions of the carbon microparticles would be like each other. Therefore, it is considered that the surface density of electric charge could be used as a specific value for a characterization of the carbon microparticles, such as preparation method and oxidized conditions of surface.

4. Conclusions

It was found that PEG 400 could be used as a dispersive reagent of carbon microparticles in a CE measurement. Carbon microparticles migrated faster toward an anode (longer migration time) with increasing its size. Many sharp peaks of the carbon microparticles on electropherogram were observed. The electropherogram of the sharp peaks corresponded to a shape of histogram on size distribution of the carbon microparticles. This shows that CE could determine the size distribution of the carbon microparticles at a short time without a measurement of SEM. Furthermore, both of the apparent electric charge q and the surface density of

electric charge of carbon microparticle were available. The apparent q value and the surface density of electric charge at 30°C for a 3.6 μm graphitic carbon microparticle were -4.4×10^{-16} C and -1.1×10^{-5} C m^{-2}, respectively. These values could be used as indices to evaluate oxidized conditions of carbons on a surface of the carbon microparticle.

This work was partly supported by a "Green and Element Chemistry" Project for Private Universities: matching fund subsidy from MEXT (Ministry of Education, Culture, Sports, Science and Technology). We thank Prof. Minoru Fukuhara of Department of Bio-applied Chemistry, Okayama University of Science (OUS), and Associate Prof. Makoto Takezaki of Department of Bio-applied Chemistry, OUS, and Associate Prof. Genta Sakane of Department of Chemistry, OUS for helpful advice on SEM, TEM, and digital microscope measurements, respectively. We also thank Mr. Hideharu Iwasaki of Kuraray Co. for gift of some carbon samples.

5. References

1) A. Chrambach, S. P. Radko, *Electrophoresis*, 2000, *21*, 259-265.

2) S. P. Radko, A. Chrambach, *Electrophoresis*, 2002, *23*, 1957-1972.

3) M. A. Rodriguez, D. W. Armstrong, *J. Chromatogr. B*, 2004, *800*, 7-25.

4) I. G. Arcibal, M. F. Santillo, A. G. Ewing, *Anal. Bioanal. Chem.*, 2007, *387*, 51-57.

5) V. Kostal, E. A. Arriaga, *Electrophoresis*, 2008, *29*, 2578-2586.

6) M. Barut, A. Podgornik, L. Urbas, B. Gabor, P. Brne, J. Vidič, S. Plevčak, A. Štrancar, *J. Sep. Sci.*, 2008, *31*, 1867-1880.

7) F.-K. Liu, *J. Chromatogr. A*, 2009, *1216*, 9034-9047.

8) N. Surugau, P. L. Urban, *J. Sep. Sci.*, 2009, *32*, 1889-1906.

9) U. Pyell, *Electrophoresis*, 2010, *31*, 814-831.

10) X. Subirats, D. Blaas, E. Kenndler, *Electrophoresis*, 2011, *32*, 1579-1590.

11) M. R. Ivanov, A. J. Haes, *Analyst*, 2011, *136*, 54-63.

12) M. Baalousha, B. Stolpe, J. R. Lead, *J. Chromatogr. A*, 2011, *1218*, 4078-4103.

13) G. Yohannes, M. Jussila, K. Hartonen, M.-L. Riekkola, *J. Chromatogr. A*, 2011, *1218*, 4104-4116.

14) S. Oszwaldowski, K. Z.-Gibula, K. P. Roberts, *Anal. Bioanal. Chem.*, 2011, *399*, 2831-2842.

15) P. S. Fedotov, N. G. Vanifatova, V. M. Shkinev, B. Y. Spivakov, *Anal. Bioanal. Chem.*, 2011, *400*, 1787-1804.

16) C. F. Duffy, K. M. Fuller, M. W. Malvey, R. O'Kennedy, E. A. Arriaga, *Anal. Chem.*, 2002, *74*, 171-176.

17) B. G. Poe, M. Navratil, E. A. Arriaga, *J. Chromatogr. A*, 2006, *1137*, 249-255.

18) J. M. Davis, E. A. Arriaga, *J. Chromatogr. A*, 2009, *1216*, 6335-6342.

19) J. Petr, O. Ryparová, J. Znaleziona, V. Maier, J. Ševčík, *Electrophoresis*, 2009, *30*, 3863-3869.

20) J. M. Davis, E. A. Arriaga, *Anal. Chem.*, 2010, *82*, 307-315.

21) H. Tang, S. Hiemstra, J. E. Thompson, *Anal. Chim. Acta*, 2011, *702*, 120-126.

22) M. Geiger, A. L. Hogerton, M. T. Bowser, *Anal. Chem.*, 2012, *84*, 577-596.

23) S.-T. Yang, X. Wang, H. Wang, F. Lu, P. G. Luo, L. Cao, M. J. Meziani, J.-H. Liu, Y. Liu, M. Chen, Y. Huang, Y.-P. Sun, *J. Phys. Chem. C*, 2009, *113*, 18110-18114.

24) S. C. Ray, A. Saha, N. R. Jana, R. Sarkar, *J. Phys. Chem. C*, 2009, *113*, 18546-18551.

25) S. N. Baker, G. A. Baker, *Angew. Chem. Int. Ed.*, 2010, *49*, 6726-6744.

26) K. Scida, P. W. Stege. G. Haby, G. A. Messina, C. D. García, *Anal. Chim. Acta*, 2011, *691*, 6-17.

27) Z. Lin, W. Xue, H. Chen, J.-M. Lin, *Anal. Chem.*, 2011, *83*, 8245-8251.

28) M. Delay, F. H. Frimmel, *Anal. Bioanal. Chem.*, 2012, *402*, 583-592.

29) G. A. P.-Trumpie, J. H. Wichers, M. Koets, L. B. J. M. Berendsen, A. van Amersongen, *Anal. Bioanal. Chem.*, 2012, *402*, 593-600.

30) F. P. Zamborini, L. Bao, R. Dasari, *Anal. Chem.*, 2012, *84*, 541-576.

31) W. Lu, X. Qin, S. Liu, G. Chang, Y. Zhang, Y. Luo, A. M. Asiri, A. O. A.-Youbi, X. Sun, *Anal. Chem.*, 2012, *84*, 5351-5357.

32) Y. Li, L. Xu, T. Chen, X. Liu, Z. Xu, H. Zhang, *Anal. Chim. Acta*, 2012, *726*, 102-108.

33) H. Liu, T. Ye, C. Mao, *Angew. Chem. Int. Ed.*, 2007, *46*, 6473-6475.

34) M. B. Müller, J. P. Quirino, P. N. Nesterenko, P. R. Haddad, S. Gambhir, D. Li, G. G. Wallace, *J. Chromatogr. A*, 2010, *1217*, 7593-7597.

35) J. Zhao, G. Chen, W. Zhang, P. Li, L. Wang, Q. Yue, H. Wang, R. Dong, X. Yan, J. Liu, *Anal. Chem.*, 2011, *83*, 9100-9106.

36) K. C. Chan, A. K. Patri, T. D. Veenstra, S. E. McNeil, H. J. Issaq, *Electrophoresis*, 2007, *28*, 1518-1524.

37) M. L.-Pastor, A. D.-Vidal, M. J. A.-Cañada, B. M. Simonet, B. Lendl, M. Valcárcel, *Anal. Chem.*, 2008, *80*, 2672-2679.

38) J. S. Baker, L. A. Colón, *J. Chromatogr. A*, 2009, *1216*, 9048-9054.

39) X. Wang, H. Bai, G. Shi, *J. Am. Chem. Soc.*, 2011, *133*,

6338-6342.

40) X. Sun, Y. Li, *Angew. Chem. Int. Ed.*, 2004, *43*, 597-601.

41) X. Sun, Y. Li, *Angew. Chem. Int. Ed.*, 2004, *43*, 3827-3831.

42) D. R. Baker, *Capillary Electrophoresis*, John Wiley and Sons, New York, 1995.

43) F.-K. Liu, G.-T. Wei, *Anal. Chim. Acta*, 2004, *510*, 77-83.

44) A. Ibrahim, H. Ohshima, S. A. Allison, H. Cottet, *J. Chromatogr. A*, 2012, *1247*, 154-164.

45) D. R. Lide (Ed.), *CRC Handbook of Chemistry and Physics*, 80th ed., CRC press, Boca Raton, FL, 1999-2000.